THE JOURNAL OF PHYSICAL CHEMISTRY B

Article

Spatiotemporal Organization of Catalysts Driven by Enhanced Diffusion

Corey Weistuch, and Steve Presse

J. Phys. Chem. B, **Just Accepted Manuscript** • DOI: 10.1021/acs.jpcb.7b06868 • Publication Date (Web): 12 Sep 2017

ACS Publications

The Journal of Physical Chemistry B is published by the American Chemical Society. 1155 Sixteenth Street N.W., Washington, DC 20036

Spatiotemporal Organization of Catalysts Driven By Enhanced Diffusion

C. Weistuch[1,2] and S. Pressé[3*†]

[1]Department of Applied Mathematics and Statistics, Stony Brook University, Stony Brook NY 11794 USA

[2]Laufer Center for Physical and Quantitative Biology, Stony Brook University, Stony Brook NY 11794 USA

[3]Department of Physics, IUPUI Indianapolis IN 46202 USA

*Corresponding author, Current address: Department of Physics and School of Molecular Sciences, Arizona State University, Tempe AZ 85287 USA

†Corresponding email: spresse@asu.edu

ABSTRACT: Recently both microfluidic and fluorescence correlation spectroscopy experiments have revealed that diffusion coefficients of active biological catalysts (enzymes) rise proportionately to their catalytic rate. Similar effects have also been observed for active material catalysts, such as platinum nanocatalysts in hydrogen peroxide solution. While differences in diffusion coefficients have recently been cleverly exploited to spatially separate active from inactive catalysts, here we investigate the consequences of these novel findings on the spatiotemporal organization of catalysts. In particular, we show that chemical reactions – such as coupled catalytic reactions – may drive effective attraction or repulsion between catalysts which in turn drives their spatiotemporal organization. This, we argue, may have implications for internal cell signaling.

I. INTRODUCTION

It is well established that active catalysts[1], such as metal catalysts half coated in platinum[2], diffuse faster in the presence of their substrate. Experiments suggest that the velocities of these catalysts grow proportionately with the amount of available substrate[2]. Similar phenomena have also been observed for other active small molecule catalysts[3] as well as active biological catalysts (enzymes) in the presence of their substrate[4–7].

For instance, fluorescence correlation spectroscopy experiments[5,7] in addition to microfluidics experiments[8], have revealed that enzymes effectively diffuse faster in the presence of their substrate with a diffusion coefficient, D, directly proportional to their reaction rate[7]. On the basis of these observations, microfluidic experiments have demonstrated that mixtures of active and inactive enzymes may be separated in physical space on the basis of catalytic activity[8].

From the simple observation that active catalysts, such as enzymes, exhibit enhanced diffusion in proportion to their catalytic rate, we construct corresponding diffusion equations describing how the evolution of an active catalyst's concentration – $E(\vec{x},t)$ – couples to the concentration of its substrate. From this we show that, under reasonable assumptions, coupled catalytic reactions – which are common for enzymatic processes – may give rise to effective attraction or repulsion between active catalysts. We show this using reaction-diffusion equations, which are used to model reactions in physical space that are especially relevant to single molecule catalysis[9], as well as other systems where reactive species are not homogeneously distributed[10–12] such as living[11,13–15] and some material[11,16] systems.

We will then briefly discuss emergent spatiotemporal ordering – of recent interest in living cells[14,17] – induced by reaction-enhanced diffusion and its potential implication on the organization of diffusing enzymes inside cells.

II. THEORY

We start from two basic experimental observations from which we construct our theory:

1) The rate of a catalytic reaction, V, depends on the amount of available substrate. That is, we assume that the rate of a catalytic reaction (the rate of product formation) is given by the following Michaelis-Menten expression

$$V = \frac{k_{cat} S^n}{K_m + S^n}. \tag{1}$$

This relation describes the phenomenon of saturation of catalysts. Here S is the substrate concentration (for which we set the units to mM), k_{cat} is the maximal turnover rate (ns^{-1}), and K_m is the Michaelis-Menten constant (mM). While Eq. (1) – with Hill coefficient, n, of unity – has been observed for enzymes that undergo enhanced

diffusion[7], Hill coefficients different from unity are easily accommodated theoretically and represent a phenomenological description of complex catalytic behaviors.

2) Experimentally, the change in the diffusion coefficient, ΔD, expressing the difference in diffusion constant in the presence (D_e, with subscript denoting "enhanced") and absence (D_0) of substrate is proportional to the reaction rate

$$\frac{\Delta D}{D_0} \propto V \rightarrow D_e = D_0 + \alpha V. \quad (2)$$

where $\Delta D > 0$ and α is an experimentally determined proportionality constant. For active catalysts, such as enzymes exhibiting enhanced diffusion, this constant is of order $0.001\mu m^2$ [7]. Furthermore, for biologically relevant examples of active enzymes such as catalase and alkaline phosphatase, respectively, we use the following parameter values ($K_m = 62mM$, $k_{cat} = 5.8 \times 10^{-5} ns^{-1}$, $\alpha \sim 0.001\mu m^2$) and ($K_m = 1.6mM$, $k_{cat} = 1.4 \times 10^{-5} ns^{-1}$, $\alpha \sim 0.0016\mu m^2$)[7].

From these observations, we now say that when acting on a single substrate, an active catalyst's concentration profile satisfies the following diffusion equation

$$\frac{\partial E(\vec{x},t)}{\partial t} = \nabla^2\Big[D_e(S(\vec{x},t))E(\vec{x},t)\Big] = \nabla^2\Big[(D_0 + \alpha V)E(\vec{x},t)\Big] \quad (3)$$

where $E(\vec{x},t)$ is the concentration, in time and space, of the active catalyst which depletes its substrate $S(\vec{x},t)$. This equation assumes that all catalysts are freely diffusing which is a reasonable assumption for small material catalysts. For large enough substrate, the catalyst-substrate complex may diffuse slower. However, for many cases, including those that we have discussed, the substrate is a small molecule and this effect may be ignored. Furthermore, $S(\vec{x},t)$, in general, satisfies its own reaction-diffusion equation.

$$\frac{\partial S}{\partial t} = D_s\nabla^2 S + E_1 V_i(S_i) - E_2 V_s(S) - \lambda S \quad (4)$$

where the substrate, S, is produced by a catalyst 1 (with concentration $E_1(\vec{x},t)$) reacting with initial substrate with concentration S_i (whose product is S) with rate $V_i(S_i)$ per catalyst. The substrate whose concentration is S may then broken down through spontaneous degradation, with first order rate constant λ, as well as by reacting with a catalyst 2 (with concentration $E_2(\vec{x},t)$) with rate $V_s(S)$ per catalyst.

For sake of clarity, and before performing any calculation, we first qualitatively observe from the form of Eq. (3) that ∇S imparts a force on an active catalyst. To see this explicitly, we write Eq. (3) as

$$\frac{\partial E}{\partial t} = (D_0 + \alpha V)\nabla^2 E + \alpha\Big[\nabla\cdot\Big(E\frac{\partial V}{\partial S}\nabla S\Big) + \frac{\partial V}{\partial S}\nabla S\cdot\nabla E\Big] \quad (5)$$

and note that the first term of Eq. (5) is simply diffusive. We then compare Eq. (5) to a Fokker-Planck equation

$$\frac{\partial E}{\partial t} = D_e\nabla^2 E - \nabla\cdot\Big(\frac{\mathbf{F}}{\zeta}E\Big) - \mathbf{v}\cdot\nabla E \quad (6)$$

We can then associate $\alpha\partial_S V(S)\nabla S$ in the second term to $-\mathbf{F}/\zeta$ where $\mathbf{F}$ is a force and ζ is a friction coefficient. Likewise, we can associate $-\alpha\partial_S V(S)\nabla S$ in the last term to a drift velocity, $\mathbf{v}$. Since both α and $\partial_S V(S)$ are strictly positive ($V(S)$ is a strictly increasing function of S), the drift velocity, or equivalently, driving force is oriented and adopts the sign of ∇S.

Furthermore, in a uniform substrate where $\nabla S = 0$, enhanced diffusion still arises through the first term of Eq. (5). However, this uniform substrate profile does not impart a net force on the active catalysts (since $\mathbf{F}$ and $\mathbf{v}$ are zero). Rather, by numerically solving coupled equations describing the evolution of the substrate and catalyst concentration, it is possible to recover times – dependent on the geometry of the volume containing the substrate and catalysts as well as initial conditions – over which ∇S may be non-zero. Furthermore, for non-zero ∇S, if the product of one catalyst becomes the substrate for another, we will see that the catalysts can effectively interact with the interaction mediated by substrate availability. The latter scenario may have implications to spatiotemporal organization inside living systems, where nonuniform steady state substrate gradients may naturally arise because proteins responsible for the generation or degradation of substrate (used by another enzyme) may themselves be spatially localized. For instance, some critical biological examples of nonuniform substrate profiles that are maintained by the spatial localization of enzymes include the regulation of cytoplasmic mRNA and protein concentrations by small GTPases (such as Ran which shuttles RNA and several proteins out of the nucleus[18]) and the regulation of hydrogen peroxide (substrate) signaling by enzymes such as catalase[19,20].

For the remainder of this paper, we will simplify our equations by introducing the following dimen-

sionless variables

$$\tilde{r}^2 = \frac{r^2}{B} \tag{7}$$

$$\tilde{t} = \frac{tD_0}{B} \tag{8}$$

$$\tilde{C} = Cr^3 \tag{9}$$

$$L = \frac{\alpha k_{cat}}{D_0} \tag{10}$$

where $\tilde{r}$, $\tilde{t}$, and $\tilde{C}$ represent dimensionless distance, time, and concentration respectively, and where L is understood as the maximal fractional change in the diffusion constant of a catalyst at saturation. As L increases, the effect of enhanced diffusion increases. As examples for biological catalysts, $L \approx 1$ for catalase and $L \approx 2.1$ for alkaline phosphatase. Furthermore, we used $B = 1\mu m^2$ since, for biological applications, this value represents a reasonable fraction of the area of a eukaryotic cell, say, where substrate concentrations may vary.

In dimensionless variables, the equations for the evolution of the second catalyst as well as the substrates S_i and S are

$$\frac{\partial \tilde{E}_2}{\partial \tilde{t}} = \tilde{\nabla}^2 \tilde{E}_2 + L_2 \tilde{\nabla}^2 \left(\frac{\tilde{E}_2 \tilde{S}^n}{K_{m2}^n + \tilde{S}^n} \right), \tag{11}$$

$$\frac{\partial \tilde{S}_i}{\partial \tilde{t}} = \frac{D_{s_i}}{D_0} \tilde{\nabla}^2 \tilde{S}_i - \frac{B}{D_0} \frac{k_{cat1} \tilde{E}_1 \tilde{S}_i^m}{K_{m1}^m + \tilde{S}_i^m} + G(\tilde{S}_i), \tag{12}$$

and

$$\frac{\partial \tilde{S}}{\partial \tilde{t}} = \frac{D_s}{D_0} \tilde{\nabla}^2 \tilde{S} + \frac{B}{D_0} \frac{k_{cat1} \tilde{E}_1 \tilde{S}_i^m}{K_{m1}^m + \tilde{S}_i^m} - \frac{B}{D_0} \frac{k_{cat2} \tilde{E}_2 \tilde{S}^n}{K_{m2}^n + \tilde{S}^n} - \frac{\lambda B}{D_0} \tilde{S}. \tag{13}$$

For generality, here we assumed the form of a Hill equation for the enzymatic rates with different Hill coefficients m and n as well as dissociation constants K_{m1} and K_{m2} for each reaction. We also assume that S_i production rate is controlled $G(\tilde{S}_i)$ which, in full generality, may depend on other reactions. In order to demonstrate that substrates can mediate catalyst attraction and repulsion, as we show shortly, we can assume for simplicity that S_i is uniform and at steady state. Furthermore, except when noted otherwise, S is assumed to be at steady state. Thus, we will be focusing on the effect of S on E_2 alone without regard for E_1 which we assume is giving rise to the concentration profile of S. Under these circumstances we will simply refer to the single catalyst species as E and the single substrate species, S.

III. RESULTS AND DISCUSSION

The first important result is that enhanced diffusion does not only affect the transient dynamics of coupled catalysts, but also affects their steady state concentration profiles as well.

To see this, we start from the steady state of Eq. (11) and consider a steady state substrate profile, $\tilde{S}$ in E. (11), to be given by either expression below

$$\tilde{S}_a = A \exp\Big(- \tilde{r}^2 \Big) \tag{14}$$

$$\tilde{S}_b = S_0 - A \exp\Big(- \tilde{r}^2 \Big). \tag{15}$$

For instance, Eq. (14) may describe the steady state of a reaction-diffusion equation with substrate primarily generated in one spatial location, followed by free diffusion of the substrate and followed by subsequent degradation or removal of the substrate over time. Eq. (15) describes a similar process with uniform generation of substrate followed by a localized depletion of substrate in one region.

In subsequent calculations, we have used $A = K_m/2$ where the active catalyst is neither over- nor under-saturated and $\tilde{r} \leq 4$ unless otherwise noted. This corresponds to an r of the order of μm [7]. For simplicity, we also assume a Hill coefficient of 1 unless otherwise noted. For a substrate – such as catalase's hydrogen peroxide for instance – we would have $A = 31mM$ while for alkaline phosphatase's substrate, $A = 0.8mM$ [7]. We also chose $S_0 = A$ as the undepleted substrate concentration in $\tilde{S}_b$.

As we now show, enhanced diffusion by catalysts affects their distribution, not only as they evolve in time, but at steady state as well. For instance, using spherical boundary conditions with $\partial_r E = 0$ at some fixed R – coinciding, for example, with the boundary of a cell in the case of a biological catalyst – we obtain the steady state distribution of catalyst from Eq. (11)

$$G = \left[1 + L \frac{\tilde{S}^n}{K_m^n + \tilde{S}^n} \right] \tilde{E} \tag{16}$$

where G is a constant that can be computed by conservation of mass.

The steady state catalyst profiles, given by

Eq. (16), and their evolution in time (starting from a delta function) are explored in Figs. (1) and (2). In particular, a substrate concentration given by Eq. (14), shown in blue in Fig. (1a), gives rise to the depletion of active catalyst, whose profile is shown in green, in the neighborhood of concentrated substrate at steady state. Thus the substrate imparts an effective force repelling the catalyst away from regions rich in substrate due to the sign of $\tilde{\nabla}\tilde{S}$ in those regions. For sake of comparison, the inactive catalyst profile is shown as a red dotted line. Fig. (1b) shows how, in the presence of open boundary conditions, the enhanced catalyst profile (green line) evolves in time by illustrating the profile at a time slice $\tilde{t} = 10$ (coinciding with a t of $\sim 100ms$ [7]) and contrasting this profile to that of the inactive catalyst profile (red line). The bimodal shape of the enhanced catalyst is reminiscent of the volcano effect seen in bacteria attempting to locate point sources of chemoattractant because the velocities of bacteria are greatest at point sources where their run over tumble probability is highest[21]. Assuming the substrate can be rapidly replenished to maintain steady state, the effect of enhanced diffusion may give rise to as much as a 50% change in concentration of catalyst over the epicenter of the concentration gradient (using parameters appropriate for alkaline phosphatase[7]).

By contrast, the profile $\tilde{S}_b$ given by Eq. (15) describes a localized depletion region which occurs if another catalyst, which depletes the substrate, is localized to one region. In this case, the opposite scenario as that predicted for profile $\tilde{S}_a$ arises. That is, active catalysts diffuse more slowly and are thus locally trapped in the depleted region as seen in Fig. (2). In other words, we see an effective attraction of active catalysts (those that generate the substrate and those that degrade the substrate) to the region depleted of substrate where the catalyst that degrades the substrate moves more slowly. Fig. (2b) shows the progression of the active catalyst profile evaluated at the same time slice as the previous figure and contrasted with the profile of the active catalyst without the depletion (red).

In order to explore the possibility of spatial organization due to enhanced diffusion, we explore Eq. (11) and Eq. (13) in their full generality. In particular, we suppose that the steady state catalyst profile in Fig. (1a) (in green) was maintained and this catalyst (catalyst 1 with dimensionless concentration $\tilde{E}_1$) also interacted with a second substrate $\tilde{S}_i$ to produce a new substrate $\tilde{S}$. This substrate could then fuel a second catalyst (catalyst 2 with dimensionless concentration $\tilde{E}_2$) which may also enhance diffuse. We would then expect

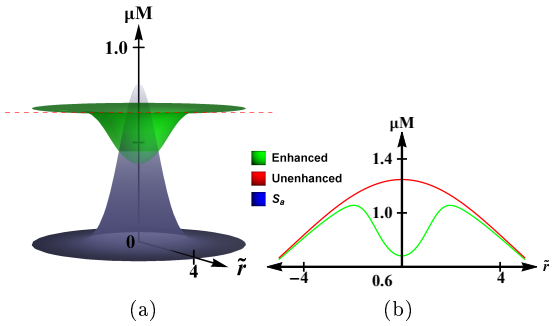

FIG. 1. **Substrate may effectively repel active catalysts in substrate rich regions** . Left: Comparison of the steady state catalyst profile when enhanced diffusion occurs (green) (projected as an (x,y) radial distribution) with the expected profile in the absence of enhancement (red) in comparison to their underlying substrate profile, S_a (blue). The substrate is rescaled to fit this plot and has a real maximum of $0.8mM$. The significant reduction in the amount of catalyst at peak substrate is easily seen. Right: At $\tilde{t} = 10$, the deviation of the enhanced diffusing catalyst (green) from normal diffusion (red) using the same substrate profile, S_a. Details of boundary conditions are explained in the main body. Concentrations are conserved in our calculations, however in the graphs it may appear otherwise; this is simply because the plots are truncated in $\tilde{r}$.

$\tilde{S}$ to be in high concentrations where catalyst 1 is present, resulting in the subsequent repulsion of catalyst 2. From this interaction, we now expect that $\tilde{E}_1$ should effectively repel $\tilde{E}_2$ due to their mutual interaction mediated through $\tilde{S}$. This is indeed recovered, as seen in Fig. (3), which shows catalyst 1 in green and catalyst 2 in magenta where we have selected $k_{cat2} = 1.0 * 10^{-7} ns^{-1}$, $K_{m2} = 6.0nM$, $\lambda = 1.0 * 10^{-4} ns^{-1} mM^{-1}$, and $D_s = 10D_0$. We also chose the constant rate of production of $\tilde{S}$ per catalyst, $V_i(S_i) = 1.4 * 10^{-9} ns^{-1} \mu M^{-1}$. Furthermore, we assumed that the total amount of both catalysts was the same, expressed in μM concentrations, as well as, chose the Hill coefficients to be 1 and 4 for the first and second catalysts, respectively. Catalyst 1 was assumed to have the same k_{cat} and K_m as alkaline phosphatase for sake of concreteness.

IV. CONCLUSION

We have drawn general predictions on effective attraction and repulsion of catalysts mediated by their substrate from a model directly inspired from experimental observations[5,7]. Our analysis predicts that enzymes within the same catalytic path-

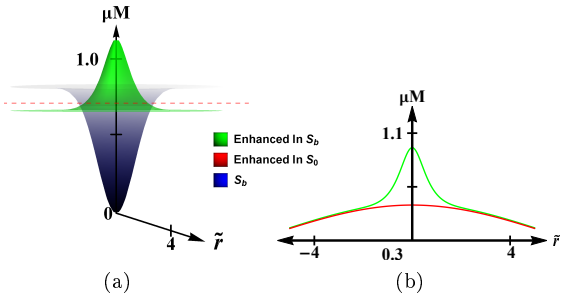

FIG. 2. **Active catalysts are effectively trapped in substrate depleted regions** . Left: Comparison of the steady state catalyst profile when enhanced diffusion occurs (green) with the expected profile, still of active catalyst, without substrate depletion (red) and in comparison to its depleted substrate profile, S_b (blue). The substrate is again rescaled to fit the plot and has a real maximum of $0.8mM$, the uniform substrate concentration if the depletion was absent. The significant buildup of catalyst near the origin is now easily seen, in direct contrast to the results of Fig. (1). Where the substrate concentration is lowest, the catalyst (green) experiences no enhancement. Right: At $\tilde{t} = 10$, the deviation of the enhanced diffusing catalyst in a depleted region (green) from its expected profile without the depletion (red) using the same substrate profile, S_b. Details of boundary conditions are explained in the main body.

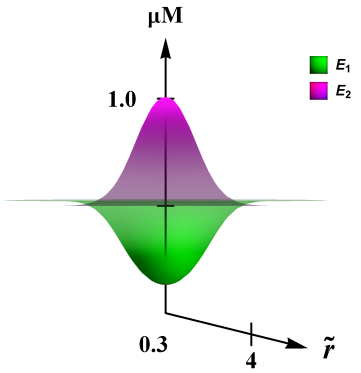

FIG. 3. **Spatial organization of catalysts due to enhanced diffusion.** Catalyst 1 (green) produces a substrate (not shown) for catalyst 2 (magenta). The regions of high substrate concentration are the regions of high catalyst 1. Due to the enhanced diffusion, catalyst 2 is repelled away from high concentrations of catalyst 1.

way or alternatively, coupled catalysts may generate forces that dramatically impact transient dynamics and ultimately influence their spatial steady state distributions.

We ignored, on physical grounds relevant to enhanced diffusion of active enzymes in experiments[7], the possibility that the catalytic activity of enzymes could heat the buffer (in which catalysts and substrate are placed) as a whole and that this heating could be responsible for the enhanced diffusion of active enzymes in experiments[7]. Indeed, if this were the case as has been incorrectly predicted in Ref.[22], physical separation of active from inactive catalysts would not be possible[8]. Furthermore, experiments directly suggest that temperature rises of the buffer are minimal, $\sim 0.2K$ [23], for typical enzyme and substrate concentrations used in experiments. This, in turn, is also consistent with the results of control experiments showing that inactive enzymes, immersed in a bath of active enzymes, are unaffected by the ongoing catalytic activity[7].

The predictions we make on the spatiotemporal organization of catalyst profiles may be tested by future experiments in microfluidic devices as already done for single enzyme diffusion[8] and may have potential implications on the distribution of enzymes sharing substrates and products as well as implications for material systems. For example, enhanced diffusion distances catalyst species from the source of their substrates perhaps providing a means to save substrate from immediate degradation Fig. (3). Furthermore, if the two catalysts produce substrate for each other – as in the well-known Goldbeter-Koshland loop[24] which describes phosphorylation and dephosphorylation loops in cells – then complex spatial modulation of substrate and catalyst distributions due to enhanced diffusion may arise. Alternatively, if two catalysts share a substrate, and at least one of them undergoes enhanced diffusion, then the two catalysts will be found in closer proximity perhaps again suggesting transient, and even stationary, spatial organization of catalytic pathways. This may also play a role in recent work on enzymatic cross-talk through competition and resource sharing[25,26].

Extending this logic further, it is now possible to imagine that the activity of a catalyst could be inferred from the dynamics of another species of catalyst and could help deduce the role of spatiotemporal ordering of biological catalysts[11,15]. As a concrete example, evidence of a "volcano-like" effect of Fig. (1) may suggest the location of a substrate-producing protein.

Recent results show that enhanced diffusion is a trait shared by several biologically crucial enzymes. In particular, malate dehydrogenase and citrate synthase, two of the enzymes in the Krebs cycle (responsible for the production of many critical high energy biomolecules), were shown to diffuse faster in the presence of their substrates[27]. It is then conceivable that this enhanced diffusion may play a role in the regulation of functional com-

plexes between these two enzymes[28]. Whether this effect is important in the crowded cellular environment and whether cells take advantage of enhanced diffusion or try to prevent it still remains to be seen.

While many of the parameters used in our simulations were inspired by work on active enzymes, our simulations are relevant to active Brownian catalysts (Figure 2 in Ref.[29]) such as self-propelled Janus catalysts[30]. More generally, our work suggests new controls to spatially and temporally manipulate catalytic processes.

V. ACKNOWLEDGEMENTS

SP would like to acknowledge support from the US Army grant "ARO 66548-EG for Complex Dynamics and Systems". CW thanks the NSF for a summer REU opportunity. We would also like to thank Dr. Konstantinos Tsekouras for interesting discussions and proof-reading this manuscript.

VI. REFERENCES

(1) Paxton, W. F.; Sundararajan, S.; Mallouk, T. E.; Sen, A. Chemical Locomotion. *Angew. Chem. Int. Ed.* **2006**, *45*, 5420–5429.
(2) Paxton, W. F.; Sen, A.; Mallouk, T. E. Motility of Catalytic Nanoparticles through Self-Generated Forces. *Chem. Eur. J.* **2005**, *11*, 6462–6470.
(3) Pavlick, R. A.; Dey, K. K.; Sirjoosingh, A.; Benesi, A.; Sen, A. A Catalytically Driven Organometallic Molecular Motor. *Nanoscale* **2013**, *5*, 1301–1304.
(4) Sengupta, S.; Dey, K. K.; Muddana, H. S.; Tabouillot, T.; Ibele, M. E.; Butler, P. J.; Sen, A. Enzyme Molecules as Nanomotors. *J. Am. Chem. Soc.* **2013**, *135*, 1406–1414.
(5) Muddana, H. S.; Sengupta, S.; Mallouk, T. E.; Sen, A.; Butler, P. J. Substrate Catalysis Enhances Single-Enzyme Diffusion. *J. Am. Chem. Soc.* **2010**, *132*, 2110–2111.
(6) Garcia-López, V.; Chiang, P.; Chen, F.; Ruan, G.; Martí, A. A.; Kolomeisky, A. B.; Wang, G.; Tour, J. M. Unimolecular Submersible Nanomachines. Synthesis, Actuation, and Monitoring. *Nano Lett.* **2015**, *15*, 8229–8239.
(7) Riedel, C.; Gabizon, R.; Wilson, C. A. M.; Hamadani, K.; Tsekouras, K.; Marqusee, S.; Pressé, S.; Bustamante, C. The Heat Released During Catalytic Turnover Enhances the Diffusion of an Enzyme. *Nature* **2015**, *517*, 227–230.
(8) Dey, K. K.; Das, S.; Poyton, M. F.; Sengupta, S.; Butler, P. J.; Cremer, P. S.; Sen, A. Chemotactic Separation of Enzymes. *ACS Nano* **2014**, *8*, 11941–11949.
(9) Gopich, I. V.; Szabo, A. Theory of the Statistics of Kinetic Transitions with Application to Single-Molecule Enzyme Catalysis. *J. Chem. Phys.* **2006**, *124*, 154712.
(10) Isaacson, S. A. A Convergent Reaction-Diffusion Master Equation. *J. Chem. Phys.* **2013**, *139*, 054101.
(11) Hellender, S.; Petzold, L. Reaction Rates for Reaction-Diffusion Kinetics on Unstructured Meshes. *J. Chem. Phys.* **2017**, *146*, 064101.
(12) Agmon, N.; Szabo, A. Theory of Reversible Diffusion-Influenced Reactions. *J. Chem. Phys.* **1990**, *92*, 5270.
(13) Paul, S.; Gangopadhyay, G. Power Law Kinetics in Reversible Enzyme-Catalyzed Reaction Due to Diffusion. *J. Chem. Phys.* **2003**, *119*, 3501.
(14) Kumar, A.; Chatterjee, S.; Nandi, M.; Dua, A. Emergence of Dynamic Cooperativity in the Stochastic Kinetics of Fluctuating Enzymes. *J. Chem. Phys.* **2016**, *145*, 085103.
(15) Buchner, A.; Tostevin, F.; Hinzpeter, F.; Gerland, U. Optimization of Collective Enzyme Activity via Spatial Localization. *J. Chem. Phys.* **2013**, *139*, 135101.
(16) Esplandiu, M. J.; Famiya, A. A.; Reguera, D. Key Parameters Controlling the Performance of Catalytic Motors. *J. Chem. Phys.* **2016**, *144*, 124702.
(17) Anderson, J. B.; Anderson, L. E.; Kussmann, J. Monte Carlo Simulations of Single- and Multistep Enzyme-Catalyzed Reaction Sequences: Effects of Diffusion, Cell Size, Enzyme Fluctuations, Colocalization, and Segregation. *J. Chem. Phys.* **2010**, *133*, 034104.
(18) Takai, Y.; Sasaki, T.; Matozaki, T. Small GTP-Binding Proteins. *Physiol. Rev.* **2001**, *81*, 153–208.
(19) Antunes, F.; Cadenas, E. Estimation of H2O2 Gradients Across Biomembranes. *FEBS Lett.* **2000**, *475*, 121–126.
(20) Stone, J. R.; Yang, S. Hydrogen Peroxide: a Signaling Messenger. *Antioxid. Redox Signal.* **2006**, *8*, 243–270.
(21) Bray, D.; Levin, M. D.; Lipkow, K. The Chemotactic Behavior of Computer-Based Surrogate Bacteria. *Curr. Biol.* **2007**, *17*, 12–19.
(22) Golestanian, R. Enhanced Diffusion of Enzymes that Catalyze Exothermic Reactions. *Phys. Rev. Lett.* **2015**, *115*, 108102.
(23) Dey, K. K.; Zhao, X.; Tansi, B. M.; Méndez-Ortiz, W. J.; Córdova-Figueroa, U. M.; Golestanian, R.; Sen, A. Micromotors Powered by Enzyme Catalysis. *Nano Lett.* **2015**, *15*, 8311–8315.
(24) Goldbeter, A.; Jr, D. E. K. An Amplified Sensitivity Arising from Covalent Modification in Biological Systems. *Proc. Natl. Acad. Sci. U.S.A.* **1981**, *78*, 6840–6844.
(25) Rondelez, Y. Competition for Catalytic Resources Alters Biological Network Dynamics. *Phys. Rev. Lett.* **2012**, *108*, 018102.
(26) Firman, T.; Ghosh, K. Competition Enhances Stochasticity in Biochemical Reactions. *J. Chem. Phys.* **2013**, *139*, 121915.
(27) Wu, F.; Pelster, L. N.; Minteer, S. D. Krebs Cycle Metabolon Formation: Metabolite Concentration Gradient Enhanced Compartmentation of Sequential Enzymes. *Chem. Commun.* **2015**, *51*, 1244–1247.
(28) Schmitt, D. L.; An, S. Spatial Organization of Metabolic Enzyme Complexes in Cells. *Biochemistry* **2017**, *56*, 3184–3196.
(29) Romanczuk, P.; Bär, M.; Ebeling, W.; Lindner, B.; Schimansky-Geier, L. Active Brownian Particles. From Individual to Collective Stochastic Dynamics. *EPJ ST* **2012**, *202*, 1–162.
(30) Zheng, X.; ten Hagen, B.; Kaiser, A.; Wu, M.; Cui, H.; Silber-Li, Z.; Löwen, H. Non-Gaussian Statistics for the Motion of Self-Propelled Janus Particles: Experiment Versus Theory. *Phys. Rev. E* **2013**, *88*, 032304.

VII. TOC GRAPHIC